SUPPLEMENTARY INFORMATION

Justification of Biowaiver and Dissolution Rate Specifications for Piroxicam Immediate Release Products Based on Physiologically Based Pharmacokinetic Modeling: An In-Depth Analysis

Xiaoting Li,[†] Yuanhang Yang,[†] Yu Zhang,[†] Chunnuan Wu,[‡] Qikun Jiang,[†] Weiping Wang,[†] Huixin Li,[†] Jing Li,[§] Cong Luo,[†] Wenying Wu,[†] Yingli Wang,[†] and Tianhong Zhang*[,†]

[†]Department of Pharmaceutical Analysis, Wuya College of Innovation, Shenyang Pharmaceutical University, No. 103, Wenhua Road, Shenyang 110016, PR China

[‡]Department of pharmacy, Tianjin Medical University Cancer Institute and Hospital, National Clinical Research Center for Cancer, Key Laboratory of Cancer Prevention and Therapy, Tianjin's Clinical Research Center for Cancer, Tianjin 300060, PR China

[§]Liaoning Key Laboratory of Environmental Pollution and Microecology, School of Basic Medical Science, Shenyang Medical College, No. 146 Huanghe North Street, Shenyang 110016, PR China

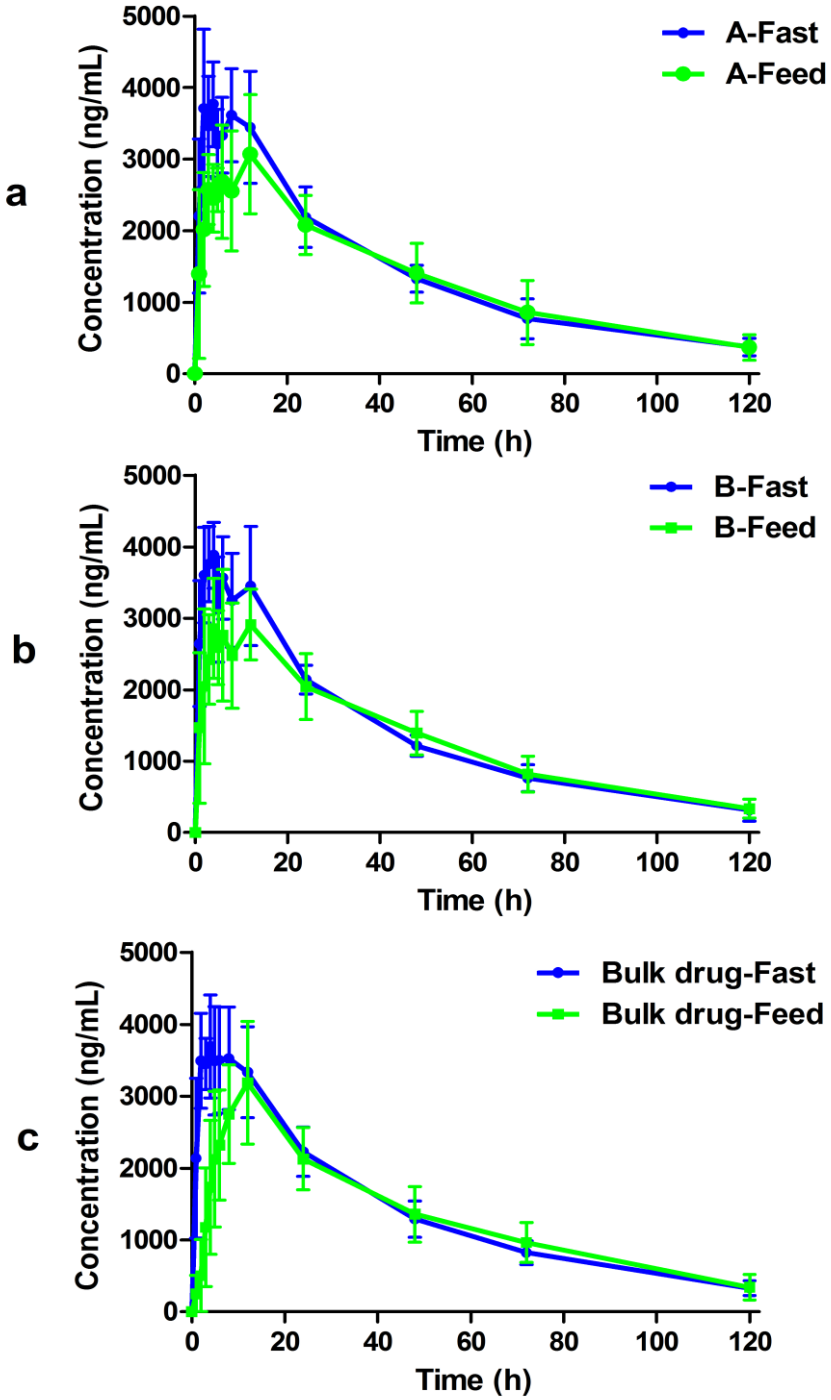

16

17 **Figure S1.** Mean plasma concentration–time curves of PIRO in beagle dogs after a single oral

18 adminstration of PIRO tablet A (a), tablet B (b) and solid bulk drug (c) in the state of feeding or

19 fasting (data were expressed as the means ± SD, n = 9).

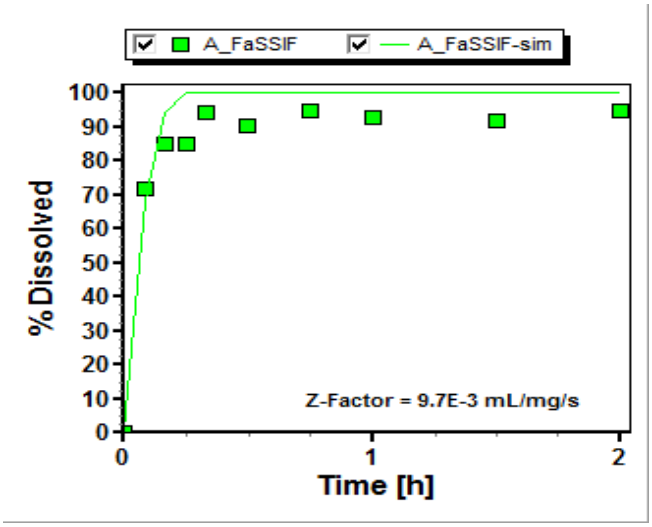

Figure S2. The graph of dissolution fitting for tablet A in FaSSIF at 75 rpm.

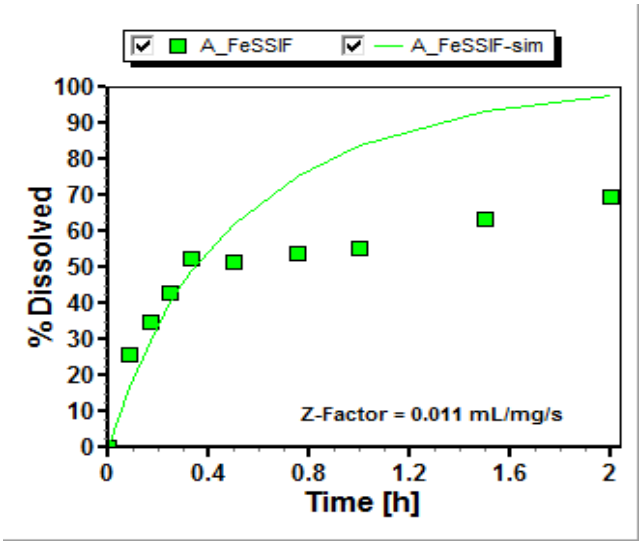

Figure S3. The graph of dissolution fitting for tablet A in FeSSIF at 75 rpm.

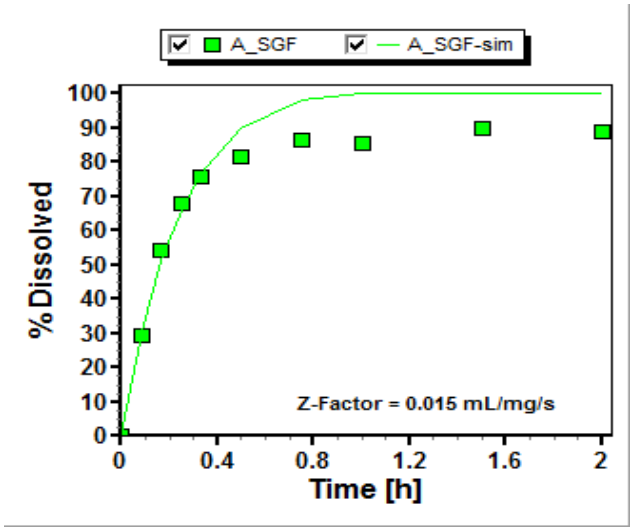

Figure S4. The graph of dissolution fitting for tablet A in SGF at 75 rpm.

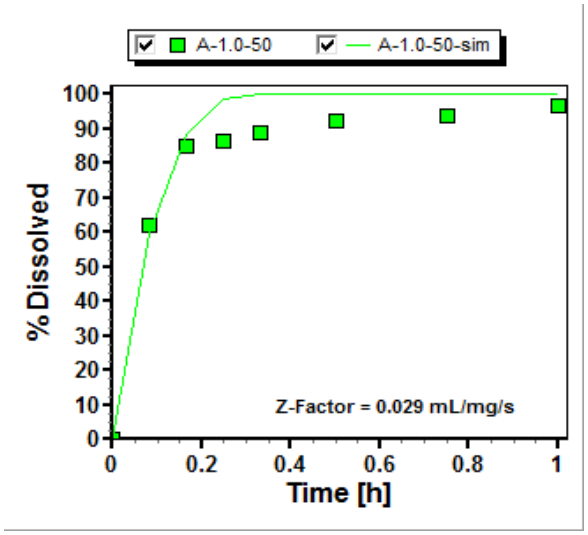

Figure S5. The graph of dissolution fitting for tablet A in 0.1 M HCl solution at 50 rpm.

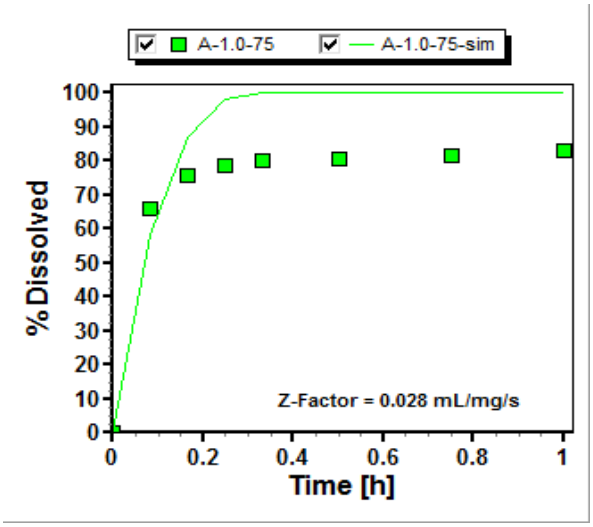

Figure S6. The graph of dissolution fitting for tablet A in 0.1 M HCl solution at 75 rpm.

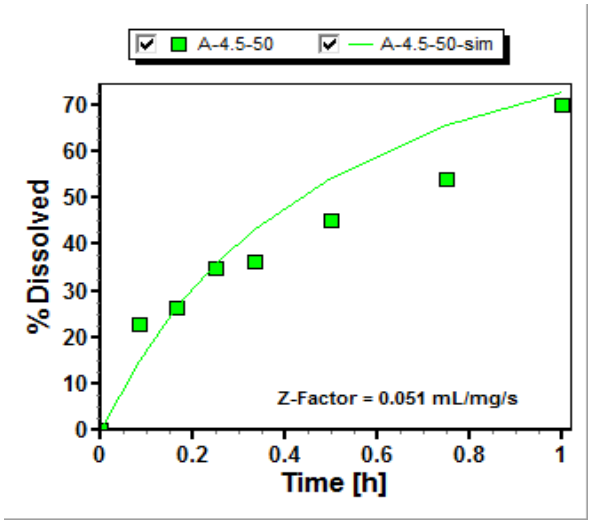

Figure S7. The graph of dissolution fitting for tablet A in pH 4.5 acetate buffer at 50 rpm.

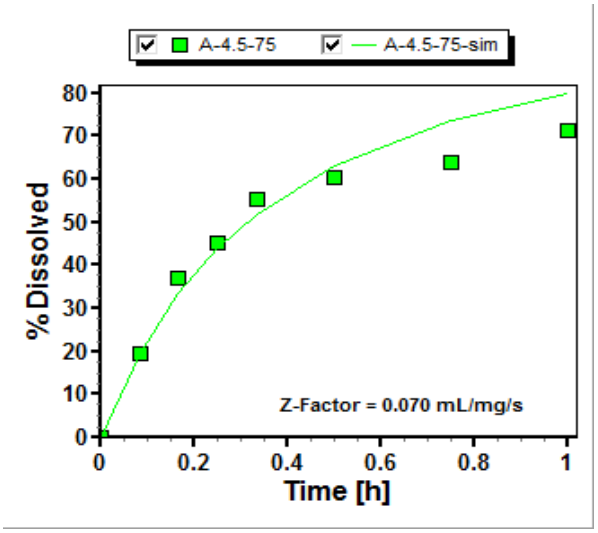

Figure S8. The graph of dissolution fitting for tablet A in pH 4.5 acetate buffer at 75 rpm.

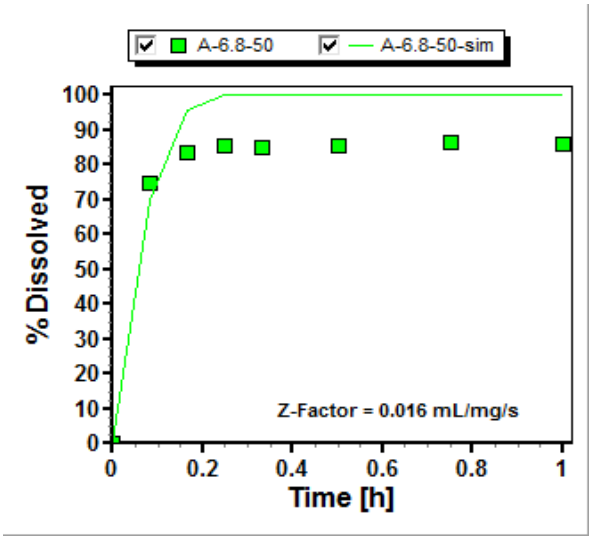

Figure S9. The graph of dissolution fitting for tablet A in pH 6.8 phosphate buffer at 50 rpm.

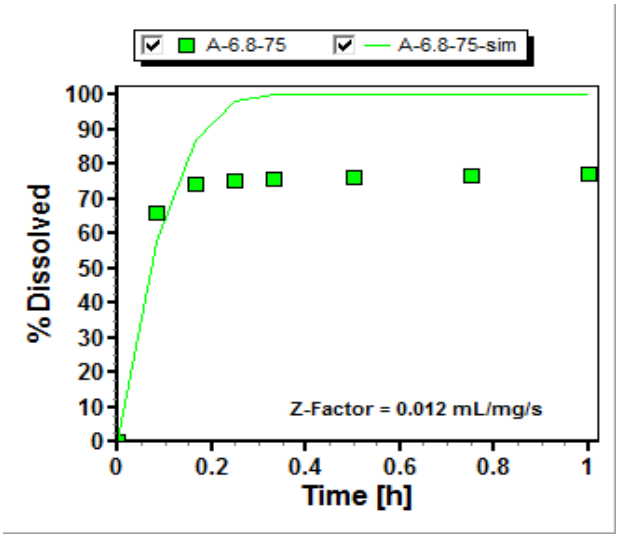

Figure S10. The graph of dissolution fitting for tablet A in pH 6.8 phosphate buffer at 75 rpm.

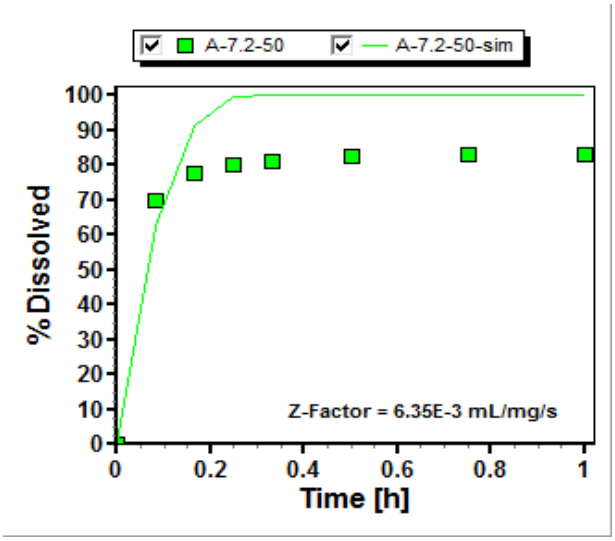

Figure S11. The graph of dissolution fitting for tablet A in pH 7.2 phosphate buffer at 50 rpm.

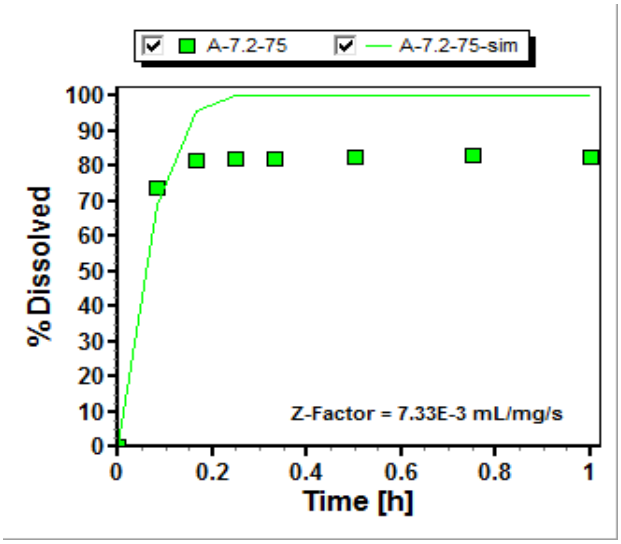

Figure S12. The graph of dissolution fitting for tablet A in pH 7.2 phosphate buffer at 75 rpm.

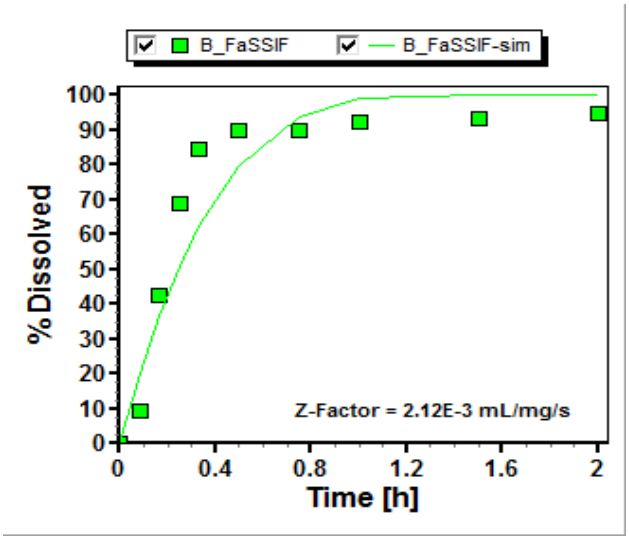

Figure S13. The graph of dissolution fitting for tablet B in FaSSIF at 75 rpm.

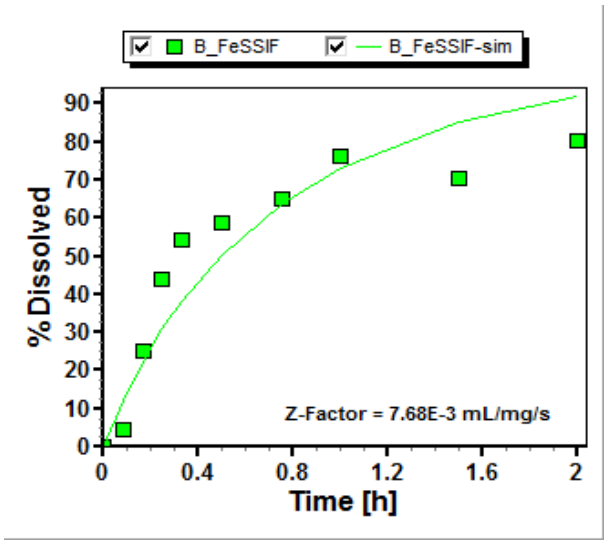

Figure S14. The graph of dissolution fitting for tablet B in FeSSIF at 75 rpm.

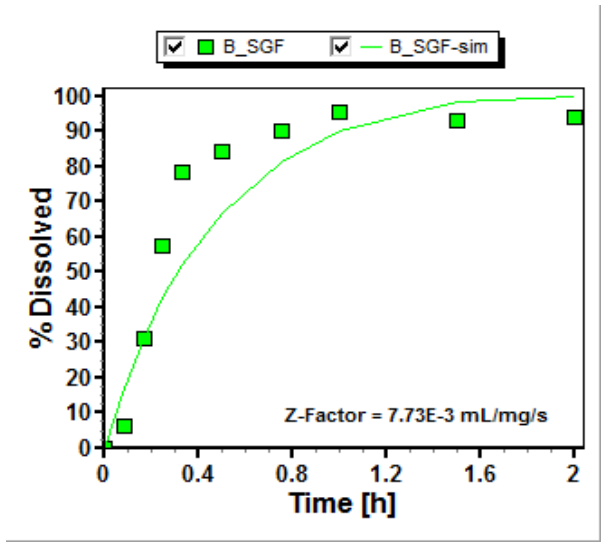

Figure S15. The graph of dissolution fitting for tablet B in SGF at 75 rpm.

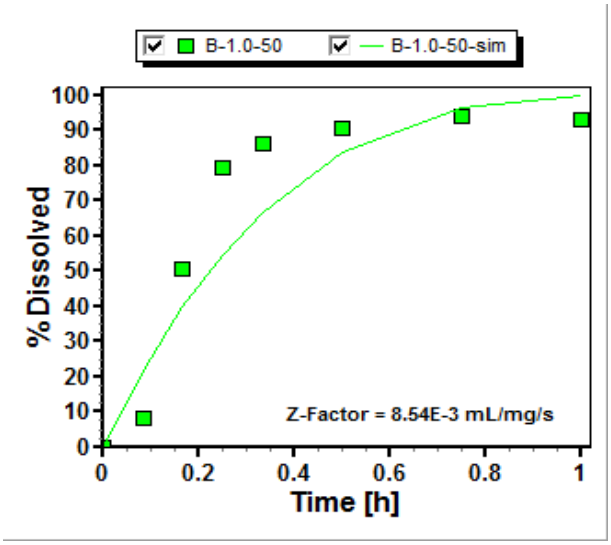

Figure S16. The graph of dissolution fitting for tablet B in 0.1 M HCl solution at 50 rpm.

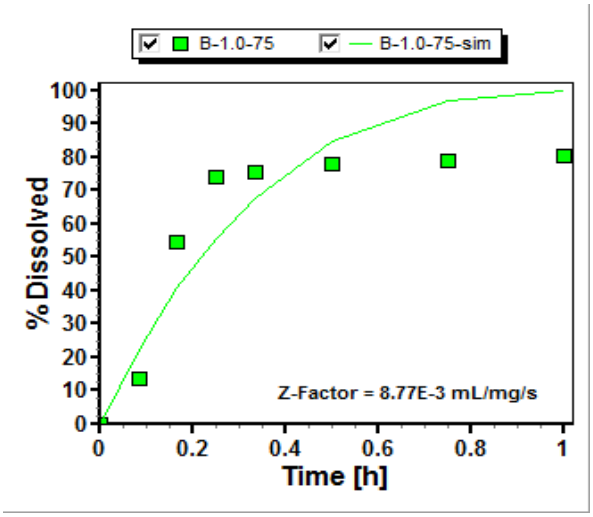

Figure S17. The graph of dissolution fitting for tablet B in 0.1 M HCl solution at 75 rpm.

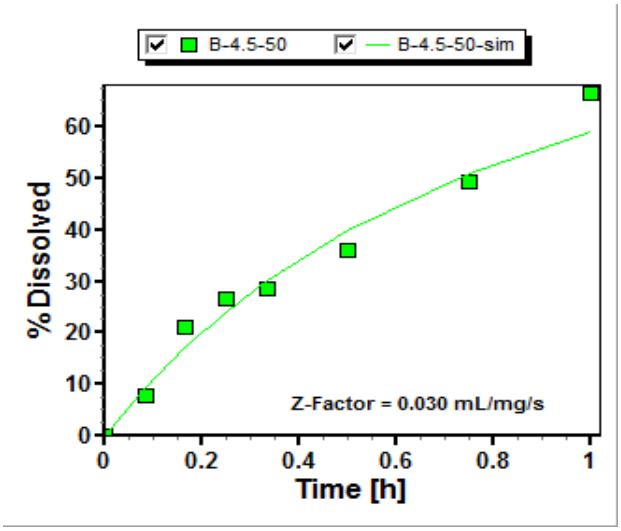

Figure S18. The graph of dissolution fitting for tablet B in pH 4.5 acetate buffer at 50 rpm.

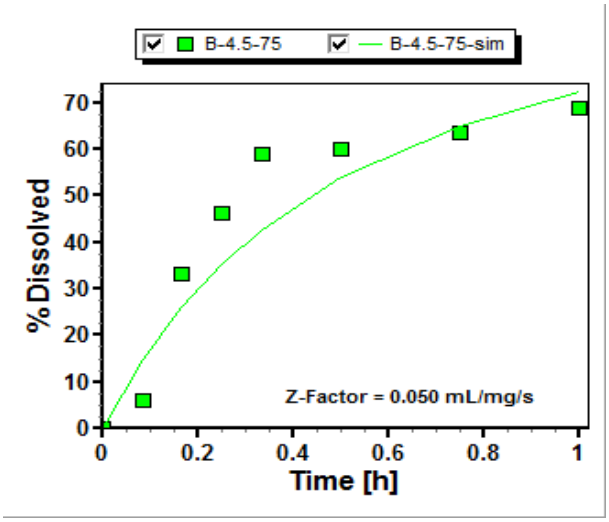

Figure S19. The graph of dissolution fitting for tablet B in pH 4.5 acetate buffer at 75 rpm.

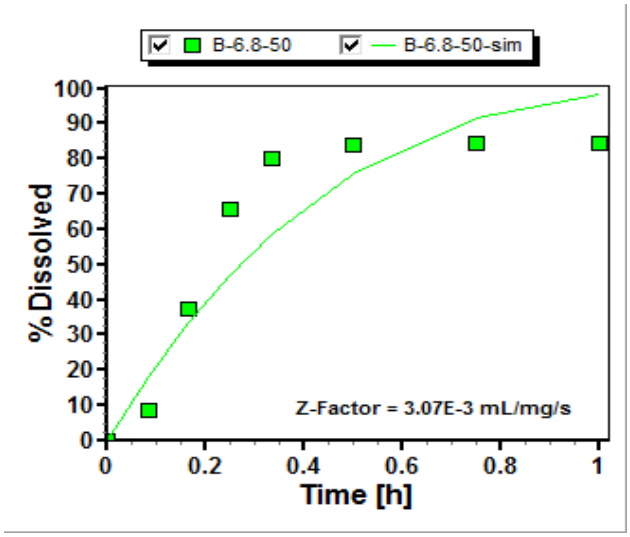

Figure S20. The graph of dissolution fitting for tablet B in pH 6.8 phosphate buffer at 50 rpm.

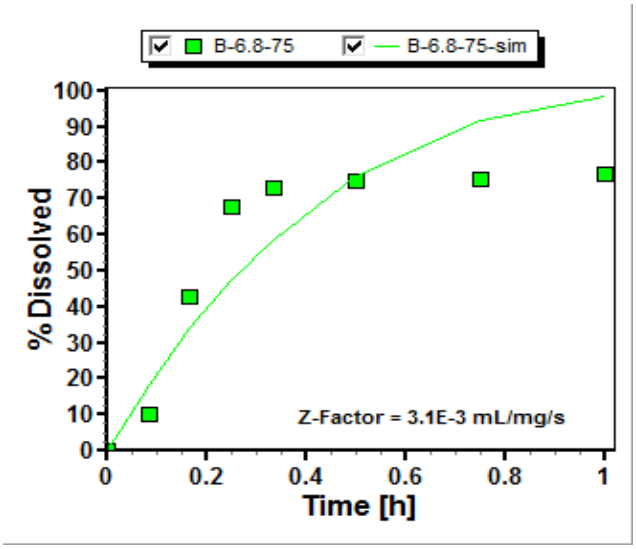

Figure S21. The graph of dissolution fitting for tablet B in pH 6.8 phosphate buffer at 75 rpm.

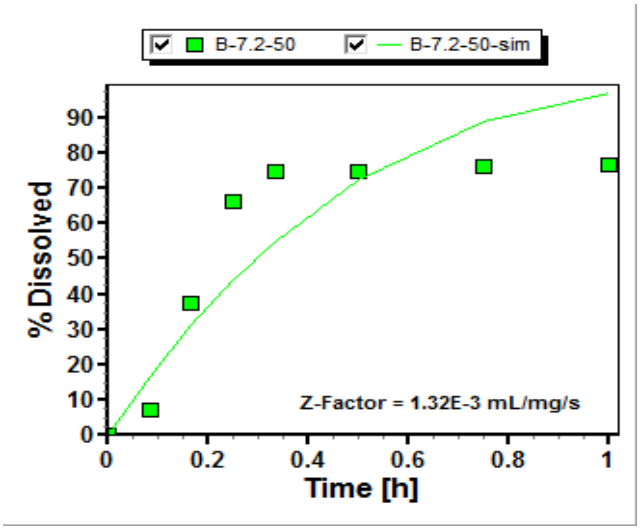

Figure S22. The graph of dissolution fitting for tablet B in pH 7.2 phosphate buffer at 50 rpm.

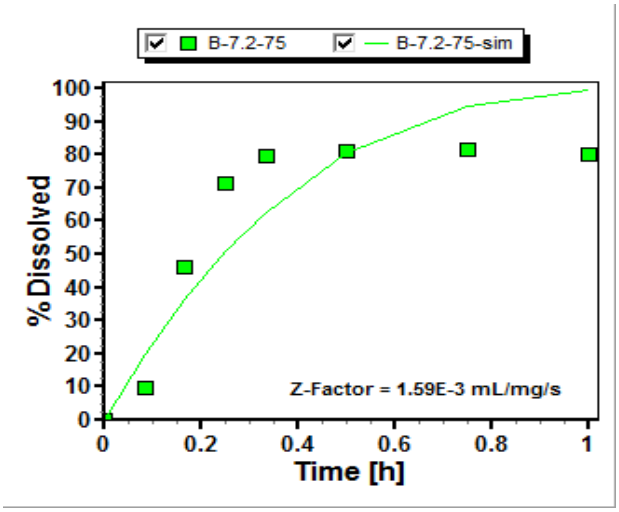

Figure S23. The graph of dissolution fitting for tablet B in pH 7.2 phosphate buffer at 75 rpm.

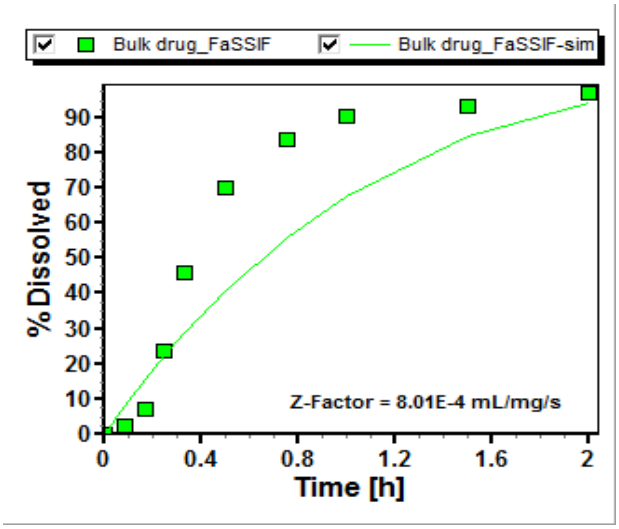

Figure S24. The graph of dissolution fitting for bulk drug in FaSSIF at 75 rpm.

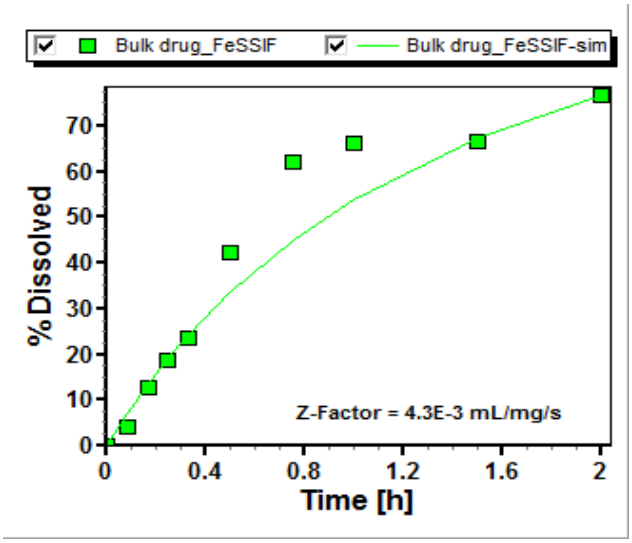

Figure S25. The graph of dissolution fitting for bulk drug in FeSSIF at 75 rpm.

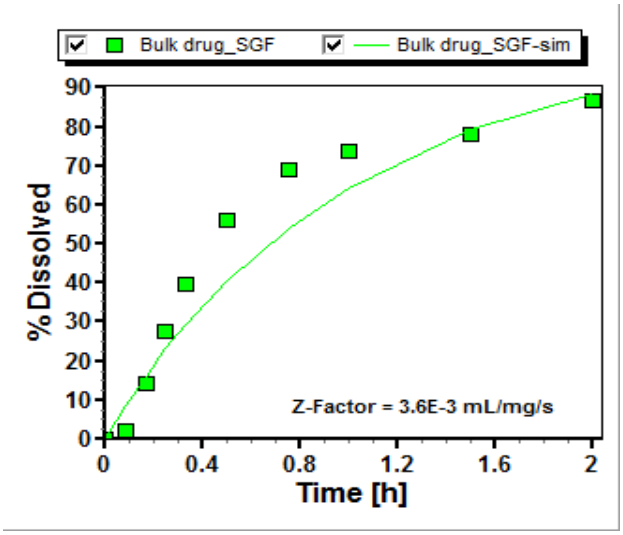

Figure S26. The graph of dissolution fitting for bulk drug in SGF at 75 rpm.

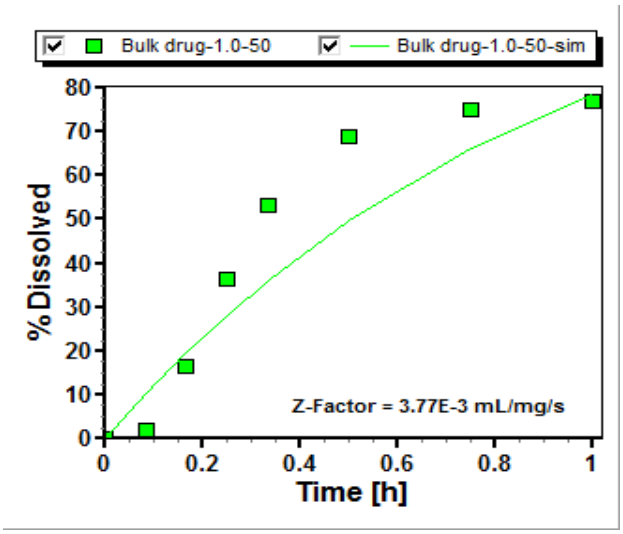

Figure S27. The graph of dissolution fitting for bulk drug in 0.1 M HCl solution at 50 rpm.

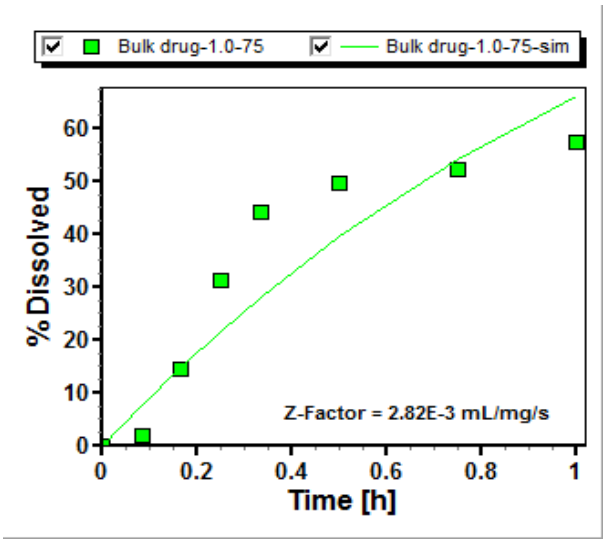

Figure S28. The graph of dissolution fitting for bulk drug in 0.1 M HCl solution at 75 rpm.

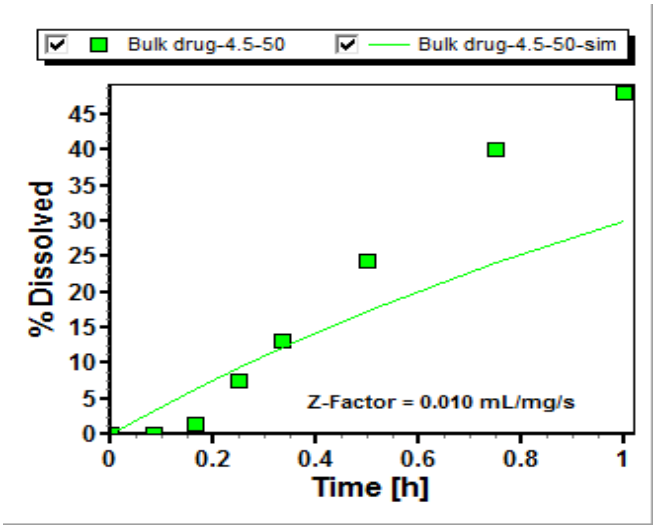

Figure S29. The graph of dissolution fitting for bulk drug in pH 4.5 acetate buffer at 50 rpm.

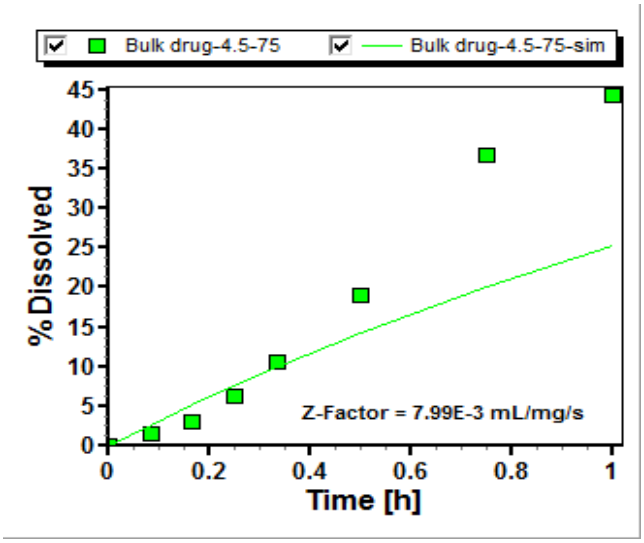

Figure S30. The graph of dissolution fitting for bulk drug in pH 4.5 acetate buffer at 75 rpm.

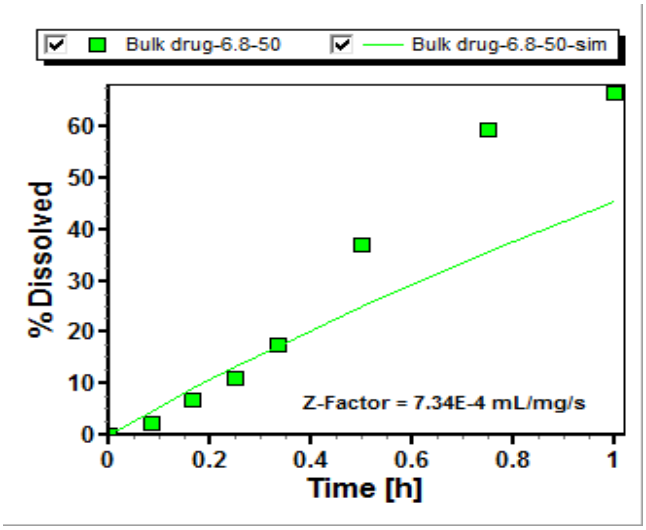

Figure S31. The graph of dissolution fitting for bulk drug in pH 6.8 phosphate buffer at 50 rpm.

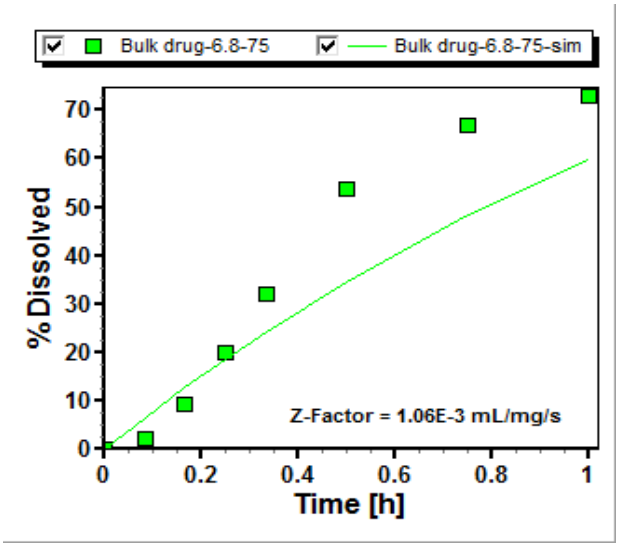

Figure S32. The graph of dissolution fitting for bulk drug in pH 6.8 phosphate buffer at 75 rpm.

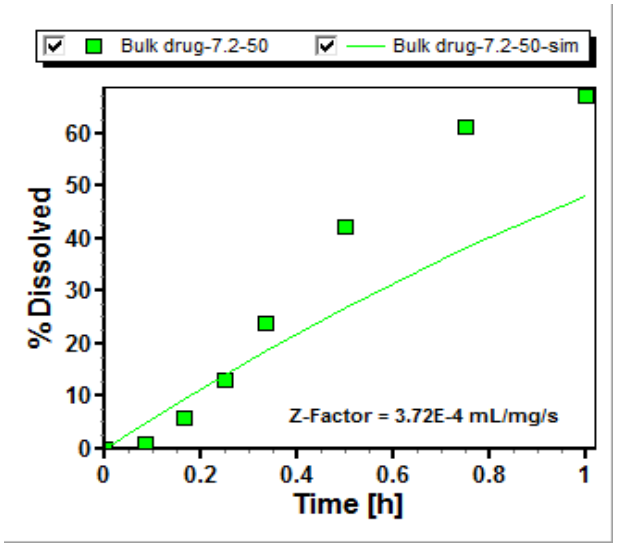

Figure S33. The graph of dissolution fitting for bulk drug in pH 7.2 phosphate buffer at 50 rpm.

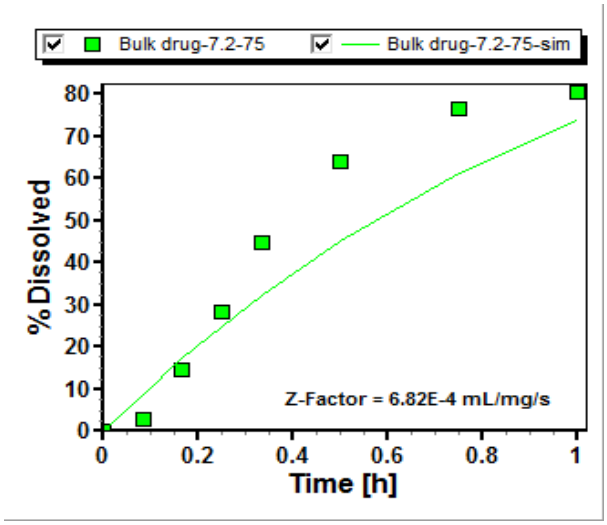

Figure S34. The graph of dissolution fitting for bulk drug in pH 7.2 phosphate buffer at 75 rpm.

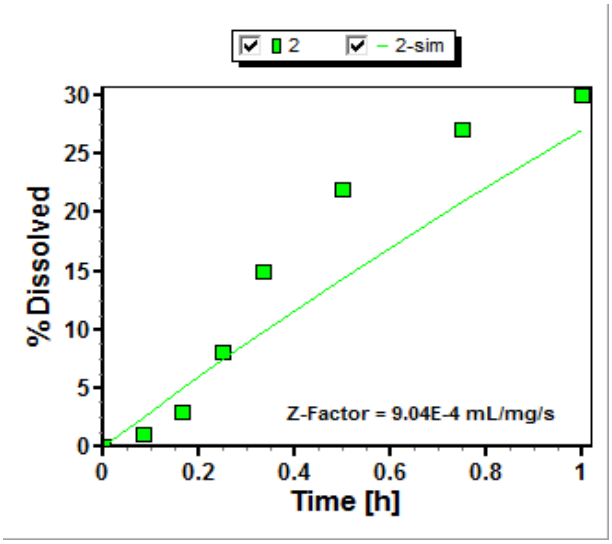

Figure S35. The graph of dissolution fitting for virtual PIRO dissolution profile (L2).

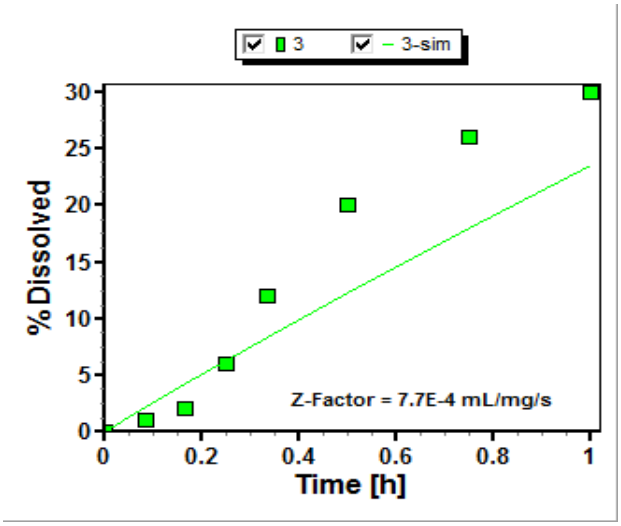

Figure S36. The graph of dissolution fitting for virtual PIRO dissolution profile (L3).

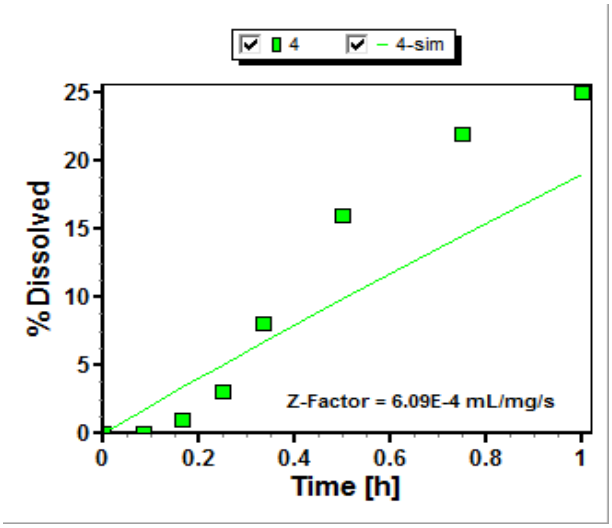

Figure S37. The graph of dissolution fitting for virtual PIRO dissolution profile (L4).

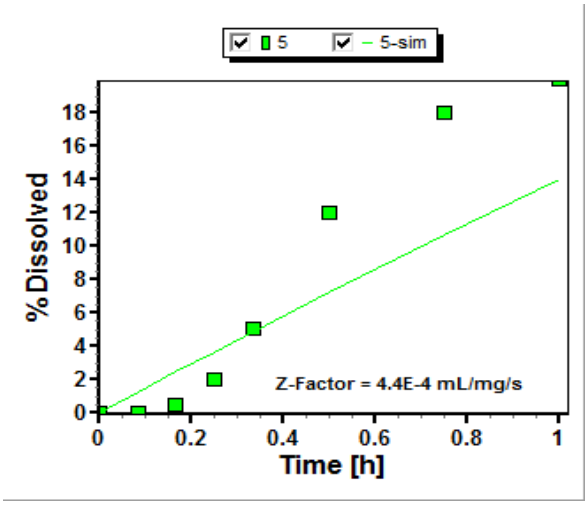

Figure S38. The graph of dissolution fitting for virtual PIRO dissolution profile (L5).

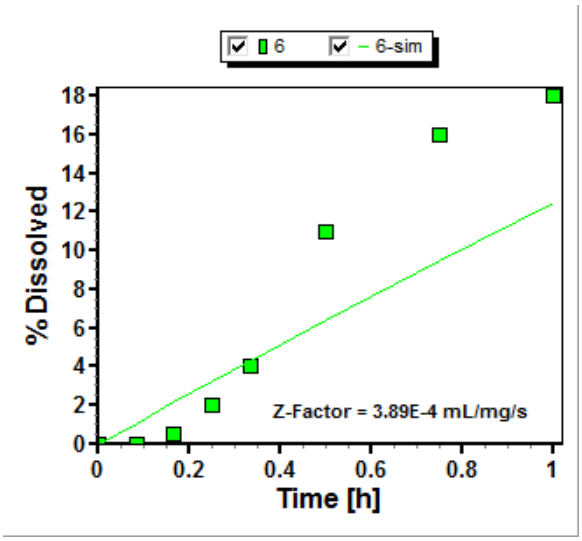

Figure S39. The graph of dissolution fitting for virtual PIRO dissolution profile (L6).

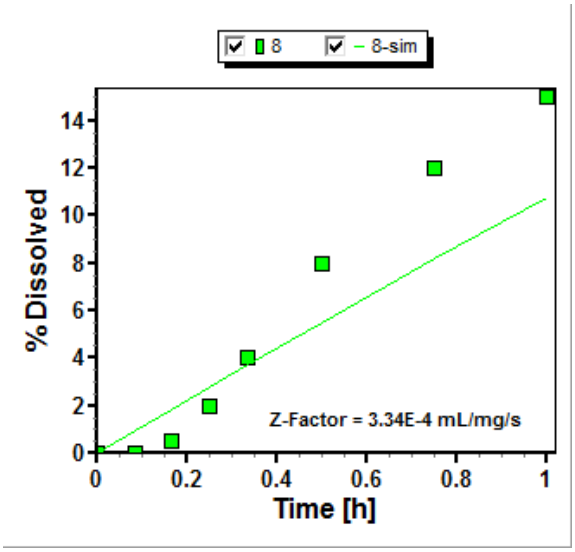

Figure S40. The graph of dissolution fitting for virtual PIRO dissolution profile (L8).

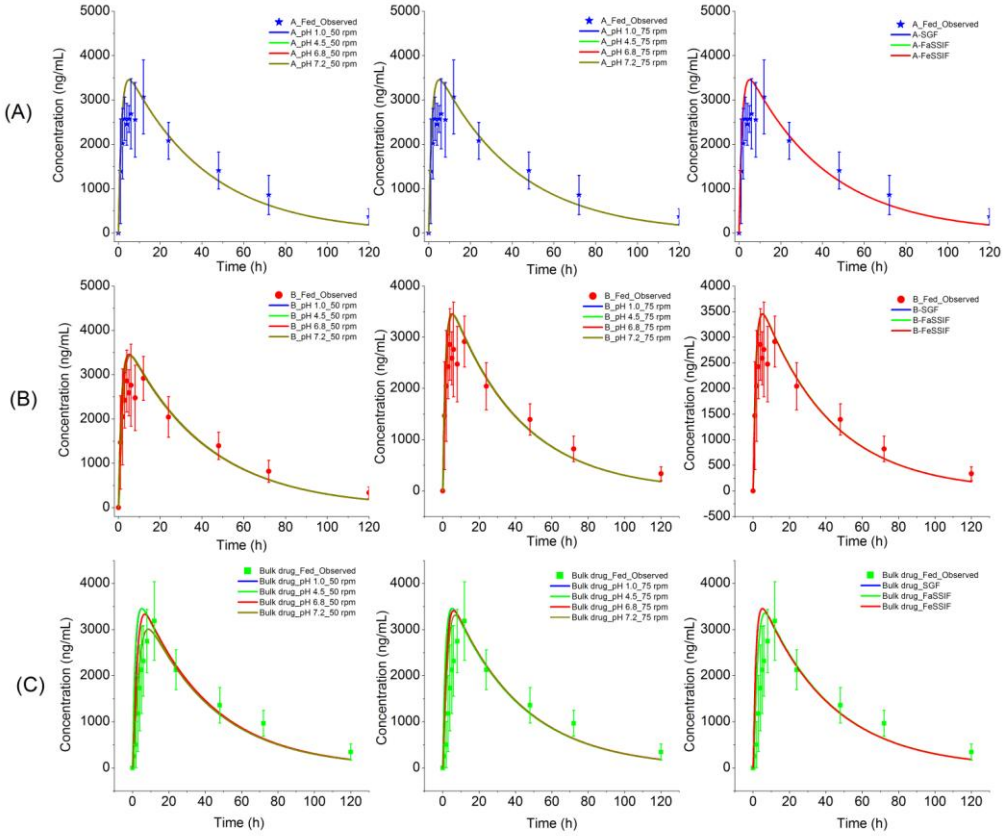

Figure S41. Predicted PK profiles in the fed beagle dogs PBPK model using Z-factor values as inputs, which were obtained by fitting to in vitro dissolution profiles under various dissolution conditions. The lines represent the predicted PK profiles and dots represent the measured ones. (A) tablet A, (B) table B and (C) solid bulk drug.

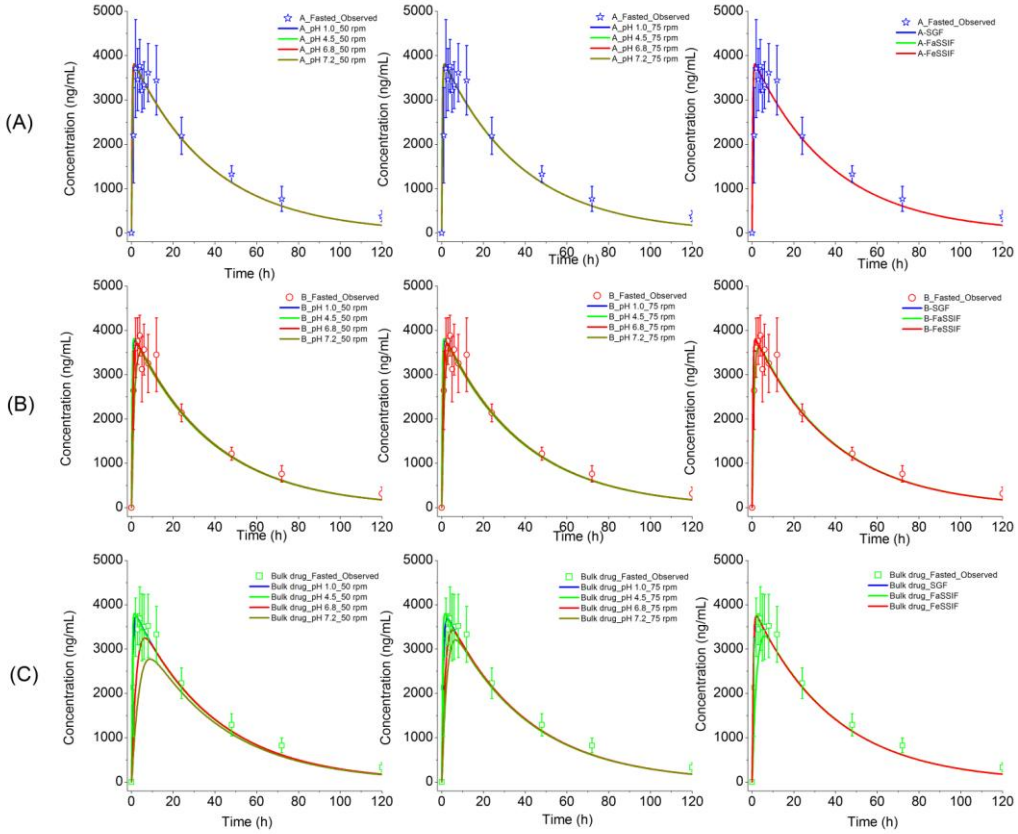

Figure S42. Predicted PK profiles in the fasted beagle dogs PBPK model using Z-factor values as inputs, which were obtained by fitting to in vitro dissolution profiles under various dissolution conditions. The lines represent the predicted PK profiles and dots represent the measured ones. (A) tablet A, (B) table B and (C) solid bulk drug.

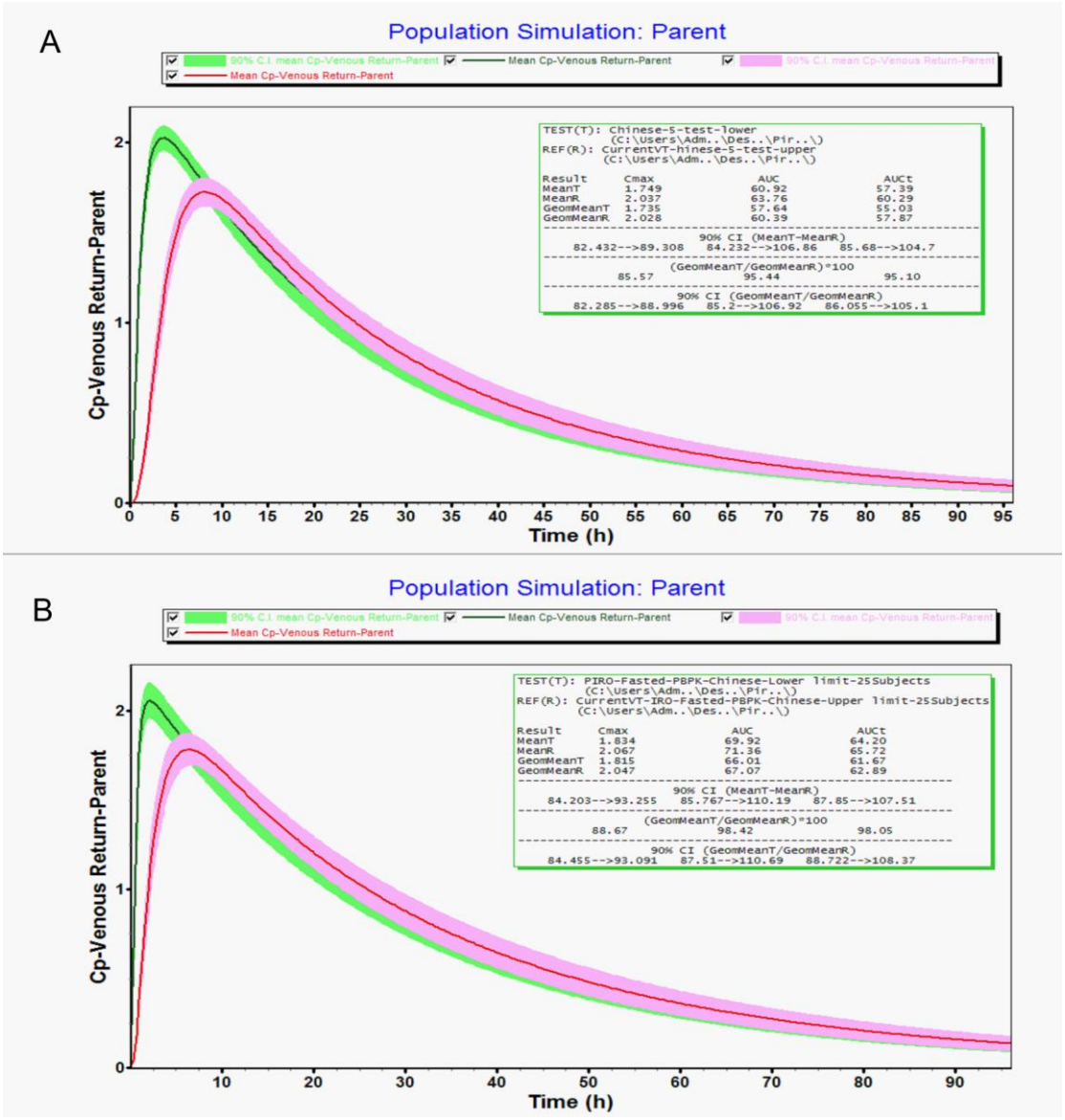

Figure S43. Virtual bioequivalence study of the reference (with the input of the upper limit virtual dissolution profiles) and the test (with the input of the lower limit virtual dissolution profiles) in 25 Chinese people. (A) fed state for L5 and (B) fasted state for L3.

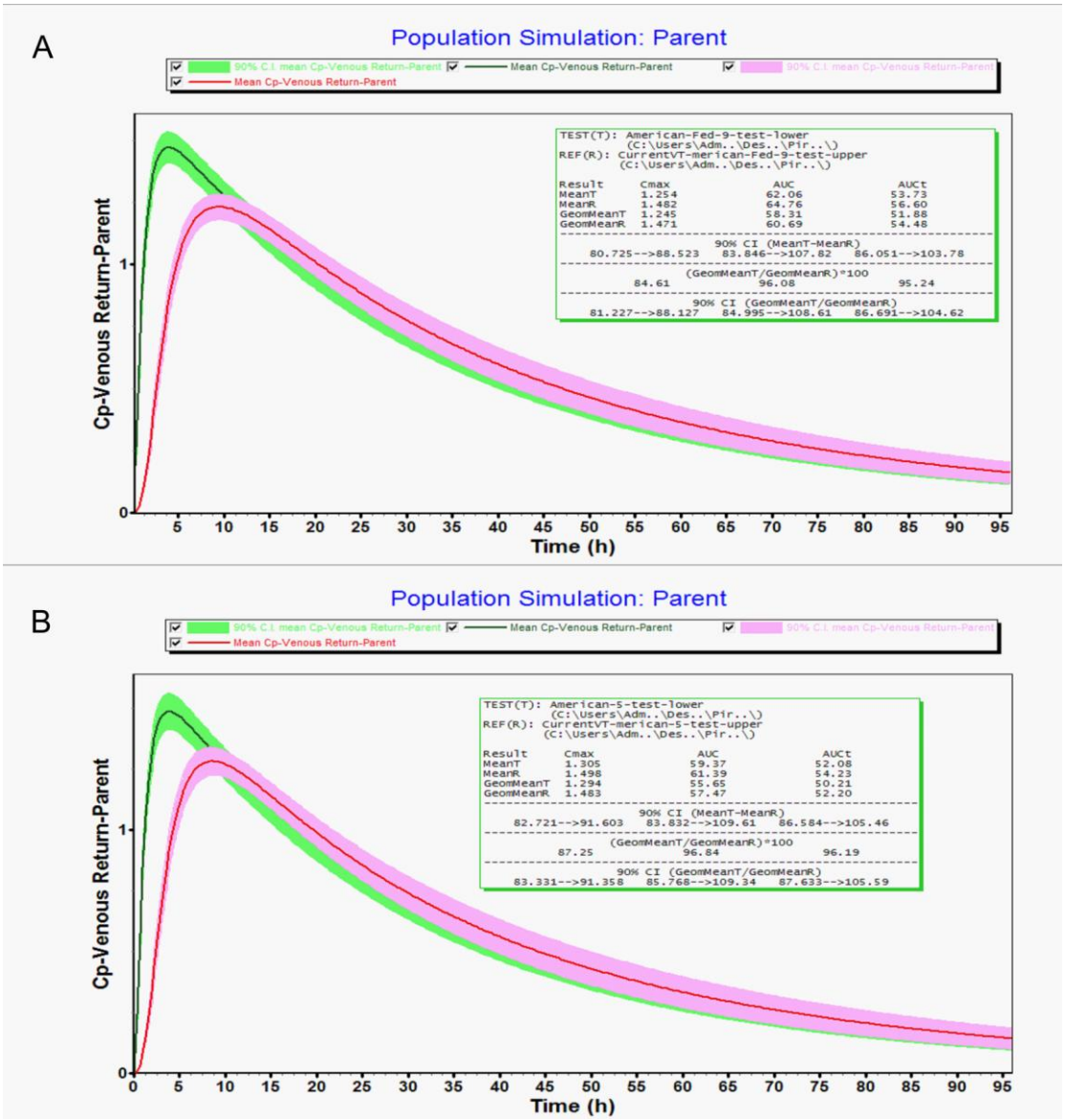

Figure S44. Virtual bioequivalence study of the reference (with the input of the upper limit virtual dissolution profiles) and the test (with the input of the lower limit virtual dissolution profiles) in 25 American people. (A) fed state for L8 and (B) fasted state for L5.

Table S1. Correlation Coefficient (R^2) and Dissolution Rate Constant (k) of PIRO Tablets A, B and Solid Bulk Drug in Different Dissolution Media including Biorelevant Media (SGF, FaSSIF and FeSSIF) and Aqueous Media at Different pH Values under Different Agitation Parameters

agitation (rpm)	media	bulk drug		A		B		dissolution rate
		R^2	k	R^2	k	R^2	k	
50	1.0	0.9699	0.0880	0.9178	0.1559	0.9673	0.1087	A > B > bulk drug
	4.5	0.8929	0.0240	0.9704	0.0302	0.9803	0.0286	A > B > bulk drug
	6.8	0.8923	0.0682	0.9777	0.3001	0.9438	0.1766	A > B > bulk drug
	7.2	0.9211	0.0700	0.9213	0.2096	0.9005	0.1246	A > B > bulk drug
75	1.0	0.9414	0.0620	0.9358	0.1905	0.9372	0.1352	A > B > bulk drug
	4.5	0.9247	0.0187	0.9548	0.0640	0.9076	0.0624	A > B > bulk drug
	6.8	0.9407	0.0578	0.9300	0.2455	0.9517	0.1453	A > B > bulk drug
	7.2	0.9536	0.0689	0.9423	0.3051	0.9559	0.1824	A > B > bulk drug
75	SGF	0.9866	0.0164	0.9797	0.0316	0.9556	0.0305	A > B > bulk drug
	FaSSIF	0.8231	0.0134	0.8042	0.1247	0.9292	0.0484	A > B > bulk drug
	FeSSIF	0.9907	0.0419	0.9835	0.0287	0.9546	0.0262	A > B > bulk drug

A Mono-Exponential Equation (MEE) was used to calculate R^2 and k.

The MEE is shown as follows:

$$\lg(y_\infty - y) = \lg y_\infty - \frac{k}{2.303} t$$

where y_∞ represents the maximum dissolution percentage of PIRO, y is the cumulative dissolution percentage of PIRO in time t and k is the dissolution rate constant.

Table S2. Difference Factor (f_1) and Similarity Factor (f_2) Values for PIRO Tablets A, B and Solid Bulk Drug in Different Media

aqueous media	pH 1.0			pH 4.5			pH 6.8			pH 7.2		
	f_2	f_1[a]	f_1[b]	f_2	f_1[a]	f_1[b]	f_2	f_1[a]	f_1[b]	f_2	f_1[a]	f_1[b]
50 rpm												
A *vs.* B	32.2	17.0	20.5	55.3	18.2	22.3	26.7	24.1	31.8	28.4	25.6	34.5
A *vs.* bulk drug	19.4	45.6	83.9	33.9	53.6	116.0	12.8	65.8	193.0	15.1	61.5	160.0
B *vs.* bulk drug	29.5	34.6	52.9	42.1	43.3	76.2	21.5	54.9	122.0	25.2	48.2	93.1
75 rpm												
A *vs.* B	34.8	16.5	19.8	63.7	7.0	7.4	32.0	19.2	23.8	29.1	20.7	26.1
A *vs.* bulk drug	19.1	53.8	117.0	24.8	65.6	190.0	19.1	50.6	102.0	18.8	45.0	81.9
B *vs.* bulk drug	27.2	44.7	80.8	25.2	64.0	178	28.7	38.9	63.5	31.5	30.7	44.3

biorelevant media	SGF			FaSSIF			FeSSIF		
	f_2	f_1[a]	f_1[b]	f_2	f_1[a]	f_1[b]	f_2	f_1[a]	f_1[b]
75 rpm									
A *vs.* B	46.8	13.0	13.5	30.4	17.3	20.8	46.7	20.4	19.1
A *vs.* bulk drug	29.8	32.0	47.0	19.0	36.7	57.2	39.2	30.2	36.2
B *vs.* bulk drug	33.1	29.1	41.0	32.0	23.4	30.4	41.8	21.8	27.9

[a]The f_1 value is obtained when the first formulation on the left column is set as the reference.

[b]The f_1 value is obtained when the second formulation on the left column is set as the reference.

Table S3. Two One-Sided *t*-Tests Results of Key Parameters for PIRO Tablet A, B and Solid Bulk Drug in Beagle Dogs in the State of Feeding or Fasting

key parameters	bluk drug—90% CI (%)	A—90% CI (%)	B—90% CI (%)
C_{max} (ng/mL)	83.6 (75.1–93.0)	78.4 (66.1–93.0)	74.6 (66.5–83.7)
T_{max} (h)	[a]$p < 0.05$	[a]$p < 0.05$	[a]$p < 0.05$
AUC_{0-t} (ng ħ/mL)	93.2 (86.4–100.5)	93.1 (83.0–104.5)	94.2 (82.1–107.9)
$AUC_{0-\infty}$ (ng ħ/mL)	94.8 (86.9–103.3)	95.1 (82.7–109.3)	94.4 (81.2–109.8)

[a]Wilcoxon signed tests of T_{max} for tablet A, B and bulk drug, the fasted group as the reference, and $p > 0.05$ (meeting the criteria).

Table S4. Z-factor Values for the Tested Three PIRO Formulations in Different Dissolution Media under Different Agitation Settings

agitation (rpm)	media	bulk drug (mL/mg/s)	A (mL/mg/s)	B (mL/mg/s)
50	pH 1.0	$3.77 \times e^{-3}$	0.029	$8.54 \times e^{-3}$
	pH 4.5	0.010	0.051	0.030
	pH 6.8	$7.34 \times e^{-4}$	0.016	$3.07 \times e^{-3}$
	pH 7.2	$3.72 \times e^{-4}$	$6.35 \times e^{-3}$	$1.32 \times e^{-3}$
75	pH 1.0	$2.82 \times e^{-3}$	0.028	$8.77 \times e^{-3}$
	pH 4.5	$7.99 \times e^{-3}$	0.070	0.050
	pH 6.8	$1.06 \times e^{-3}$	0.012	$3.10 \times e^{-3}$
	pH 7.2	$6.82 \times e^{-4}$	$7.33 \times e^{-3}$	$1.59 \times e^{-3}$
	SGF	$3.60 \times e^{-3}$	0.015	$7.73 \times e^{-3}$
	FaSSIF	$8.01 \times e^{-4}$	$9.7 \times e^{-3}$	$2.12 \times e^{-3}$
	FeSSIF	$4.30 \times e^{-3}$	0.011	$7.68 \times e^{-3}$

Table S5. Results of the Crossover Virtual Trial Simulations for PIRO IR Products in Chinese and American (n=25) People

	Z-factor	state	90% CI	C_{max} (ng/mL)	$AUC_{0-\infty}$ (ng ħ/mL)	AUC_{0-t} (ng ħ/mL)
American–L3	$7.70\times e^{-4}$	fasted	mean (%)	89.6	99.2	98.8
			range (%)	85.8~93.6	88.3~111.4	89.8~108.7
		fed	mean (%)	94.5	98.9	98.5
			range (%)	90.0~99.3	85.4~114.6	87.9~110.3
American–L4	$6.09\times e^{-4}$	fasted	mean (%)	87.4	99.5	99.1
			range (%)	84.6~90.4	89.7~110.2	91.0~107.9
		fed	mean (%)	92.8	99.8	99.3
			range (%)	88.9~96.8	89.1~111.8	90.8~108.5
American–L5	$4.40\times e^{-4}$	fasted	mean (%)	87.3	96.8	96.2
			range (%)	83.3~91.4	85.8~109.3	87.6~105.6
		fed	mean (%)	88.3	96.8	96.3
			range (%)	84.9~91.9	86.7~108.1	88.0~105.5
American–L8	$3.34\times e^{-4}$	fasted	mean (%)	76.06	95.4	94.9
			range (%)	72.40~79.90	84.4~107.9	85.5~105.2
		fed	mean (%)	84.6	96.1	95.2
			range (%)	81.2~88.1	85.0~108.6	86.7~104.6
Chinese–L3	$7.70\times e^{-4}$	fasted	mean (%)	88.7	98.4	98.1
			range (%)	84.5~93.1	87.5~110.7	88.7~108.4
		fed	mean (%)	91.2	97.4	97.0
			range (%)	88.5~94.0	83.2~114.1	84.8~110.9
Chinese–L4	$6.09\times e^{-4}$	fasted	mean (%)	83.2	96.7	96.2
			range (%)	78.79~87.8	83.4~112.1	84.8~109.3
		fed	mean (%)	90.3	97.4	96.9
			range (%)	86.8~93.9	86.2~110.0	87.5~107.4
Chinese–L5	$4.40\times e^{-4}$	fasted	mean (%)	79.60	92.8	92.2
			range (%)	76.11~83.2	83.9~102.6	84.7~100.5
		fed	mean (%)	85.6	95.4	95.1
			range (%)	82.3~89.0	85.2~106.9	86.1~105.1
Chinese–L8	$3.34\times e^{-4}$	fasted	mean (%)	74.99	87.8	87.0
			range (%)	71.99~78.12	77.45~99.5	78.97~95.9
		fed	mean (%)	79.49	90.4	89.9
			range (%)	75.98~83.2	78.95~103.5	80.3~100.6